AIAA JOURNAL
Vol. 38, No. 5, May 2000

Interactive Physical Programming: Tradeoff Analysis and Decision Making in Multicriteria Optimization

Ravindra V. Tappeta*
General Electric Corporate R&D Center, Niskyuna, New York 12309
John E. Renaud†
University of Notre Dame, Notre Dame, Indiana 46556
and
Achille Messac‡ and Glynn J. Sundararaj§
Northeastern University, Boston, Massachusetts 02115

This research focuses on multiobjective system design and optimization. The goal is to extend the physical programming (Messac, A., "Physical Programming: Effective Optimization for Design," *AIAA Journal*, Vol. 34, No. 1, 1996, pp. 149–158). Framework to develop an interactive physical programming (IPP) framework that takes into account the designer's or the decision maker's (DM's) preferences during the optimization process, and allows for design exploration at a given Pareto design. The IPP framework provides the DM with Pareto-sensitivity information, a Pareto surface approximation, a formal decision-making strategy, and a Pareto visualization tool for efficient design (or Pareto surface) exploration at a given Pareto design. The IPP has been successfully applied to two test problems. The first problem consists of a set of simple analytical expressions for its objective and constraints. The second problem is the design and sizing of a high-performance and low-cost 10-bar structure that has multiple objectives. Results indicate that the IPP framework is effective in capturing the local preferences of the DM. The Pareto designs that reflect the DM's preferences can be efficiently generated using the IPP framework. More importantly, the IPP provides the DM with a Pareto visualization tool that facilitates the study of existing tradeoffs between objectives in a physically meaningful way.

Introduction

MANY engineering design problems are multiobjective in nature as they often involve more than one design goal. These design goals impose potentially conflicting requirements on the technical and economical performances of a given system design. To study the tradeoffs between these conflicting design goals (or objectives) and to explore available design options, one needs to formulate the optimization problem with multiple objectives (vector optimization). Vector optimization algorithms seek an optimum design that attains the multiple objectives as closely as possible whereas satisfying constraints strictly. Note that an infinite number of problem formulations are introduced to the decision maker (DM) when using vector optimization. This calls for the incorporation of Pareto optimality concepts into optimization algorithms and procedures that require the designer's involvement as a DM.[1–4]

A variety of techniques and applications of multiobjective optimization have been developed over the past few years. The progress in the field of multicriteria optimization was summarized by Hwang and Masud[5] and, later, by Stadler et al.[3] A comprehensive survey of the multiobjective optimization methods (traditional, evolutionary, and interactive) is also given in Ref. 6. Most of the traditional methods involve converting a multiobjective problem into a single-objective problem and then solving this single objective problem for a compromise solution. This scalarization is usually achieved by using either weights or targets that the designer's have to specify for each objective a priori. These weights or targets are inadequate in capturing the designer's preferences. The disadvantages of using traditional methods for multiobjective system optimization are as follows: they 1) require a priori selection of weights or targets for each of the objective functions, 2) provide information for only one design scenario (i.e., a single Pareto solution), 3) are unable to generate proper Pareto points for nonconvex problems (e.g., the weights method), 4) are incapable of generating sensitivity information for tradeoff and decision making, and 5) have no inherent capabilities for design exploration.

Problem Formulation

A general multiobjective optimization problem is to find the design variables that optimize a vector objective function ($\boldsymbol{f}(\boldsymbol{x}) = \{f_1, \ldots, f_m\}$) over the feasible design space. The objective functions are the quantities that the designer wishes to minimize, maximize, or attain a certain value. The problem formulation in standard form for a minimization is given here, and is similar for the other cases.

$$\begin{aligned} \text{Minimize:}\quad & \boldsymbol{f}(\boldsymbol{x}) = \{f_1(\boldsymbol{x}), f_2(\boldsymbol{x}), \ldots, f_m(\boldsymbol{x})\} \\ \text{Subject to:}\quad & g_k(\boldsymbol{x}) \geq 0, \qquad k = 1, \ldots, p \\ & h_j(\boldsymbol{x}) = 0, \qquad j = 1, \ldots, q \\ & x_l^u \geq x_l \geq x_l^l, \qquad l = 1, \ldots, n \end{aligned} \tag{1}$$

Pareto Optimal Concept

Following some earlier statements and discourses, Pareto in 1906 provided a final statement on the optimality concept of multiobjective problems in the context of welfare economics. Pareto optimality serves as the basic multicriteria optimization concept in virtually all of the research literature. The Pareto optimality concept for multiobjective optimization is similar to what the Karush Kuhn-Tucker (KKT) conditions are for a single objective optimization problem. The Pareto optimality concept is stated as follows: A vector of $\boldsymbol{x}^*$ is Pareto optimal if there exists no feasible vector $\boldsymbol{x}$ that would decrease some objective function without causing a simultaneous increase in

Received 25 March 1999; presented as Paper 99-1209 at the AIAA/ASME/ASCE/AHS/ASC 40th Structures, Structural Dynamics, and Materials Conference, St. Louis, MO, 12–15 April 1999; revision received 14 September 1999; accepted for publication 16 September 1999.

*Mechanical Engineer, Engineering Mechanics Laboratory. Member AIAA.
†Associate Professor, Aerospace and Mechanical Engineering. Associate Fellow AIAA.
‡Associate Professor, Mechanical Engineering. Associate Fellow AIAA.
§Associate Professor, Mechanical Engineering.

at least one objective function. Mathematically, the Pareto optimality is defined as follows: A vector of $\boldsymbol{x}^*$ is a Pareto optimum iff, for any $\boldsymbol{x}$ and i,

$$f_j(\boldsymbol{x}) \le f_j(\boldsymbol{x}^*), \qquad j = 1, \ldots, m, \qquad j \ne i \Longrightarrow f_i(\boldsymbol{x}) \ge f_i(\boldsymbol{x}^*) \tag{2}$$

Physical Programming

This section briefly describes a method called physical programming (PP) that is suitable for generating a preferred Pareto (or compromise) design during multiobjective system design and optimization. PP captures the designer's preferences a priori in a mathematically consistent manner using preference functions. The application of PP does not require the designer to specify weights for each objective function. Rather, the designer specifies ranges of differing degrees of desirability for each objective function. The initial development of the PP methodology is presented in Ref. 7, with a structural application example. Other applications of PP include high-speed-civil-transport plane design[8] and robust control design.[9] In PP, the designer classifies objective functions into the following four different categories:

Class 1-S—Smaller-Is-Better (i.e., Minimization)
Class 2-S—Larger-Is-Better (i.e., Maximization)
Class 3-S—Value-Is-Better (i.e., Seek Value)
Class 4-S—Range-Is-Better (i.e., Seek Range)

The qualitative meaning of preference function is depicted in Fig. 1. The value of the objective function, f_i, is on the horizontal axis, and the function that is minimized for that objective, p_i, called the preference function, is on the vertical axis. The system aggregate objective function is formed based on the preference functions and not on the objective functions. These preference functions provide the means for the DM to express ranges of differing levels of preferences, within each given objective function.

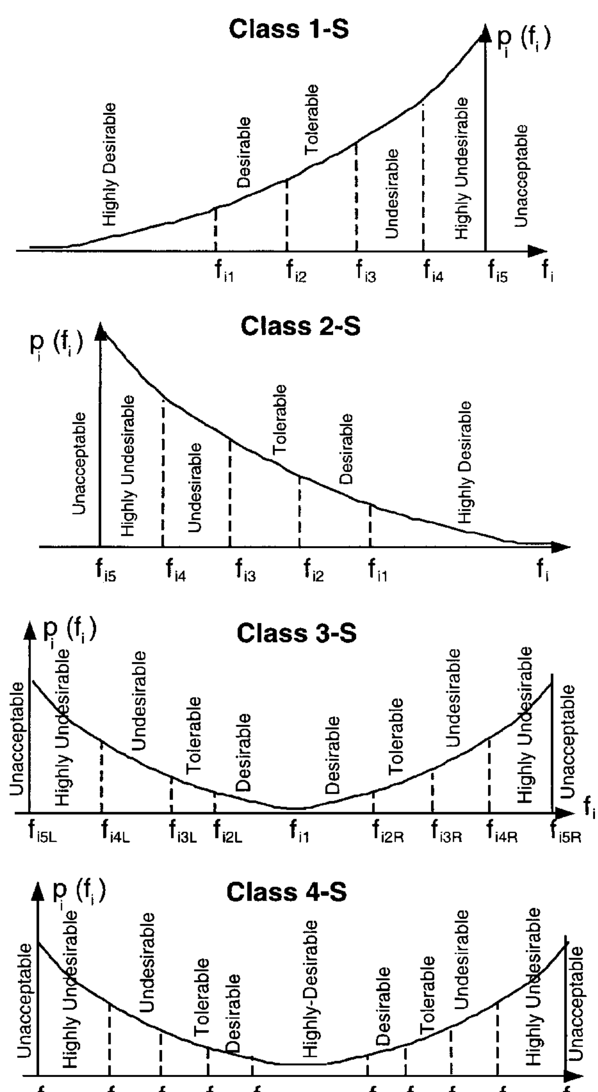

Fig. 1 Objective function space.

The DM specifies his/her preference for each given objective function. The PP lexicon comprises terms that characterize the degree of preference associated with six ranges for each generic objective function. For classes 1-S and 2-S, there are six ranges, ten ranges for class 3-S, and 11 for class 4-S. For illustration, consider the case of class 1-S, shown in Fig. 1. The ranges are defined as follows, in order of decreasing preference.

Highly desirable (h) range ($f_i \le f_{i1}$): An acceptable range over which the improvement that results from further reduction of the preference metric is desired, but is of minimal additional value.

Desirable (D) range ($f_{i1} \le f_i \le f_{i2}$): An acceptable range that is desirable.

Tolerable (T) range ($f_{i2} \le f_i \le f_{i3}$): An acceptable, tolerable range.

Undesirable (U) range ($f_{i3} \le f_i \le f_{i4}$): A range that, although acceptable, is undesirable.

Highly undesirable (H) range ($f_{i4} \le f_i \le f_{i5}$): A range that, although still acceptable, is highly undesirable.

Unacceptable (UA) range ($f_{i5} \le f_i$): The range of values that the objective function may not take.

The parameters f_{i1} through f_{i5} are physically meaningful values that are specified by the DM to quantify the preference functions associated with the ith objective. These parameters delineate the different preference ranges for each objective function. The quantitative mathematical implications of the above definitions and mathematical means for the development of the class function for each objective are given in Messac.[7] Once the range parameters are defined for each objective function, preference functions are constructed. In this research, the initial Pareto design that best satisfies the DM's preferences is generated by solving the following compromise programming (CP) problem.[10]

$$\text{Minimize:} \quad P(\boldsymbol{f}(\boldsymbol{X})) = z + \alpha \sum_{i=1}^{m} p_i(f_i)$$

$$\text{Subject to:} \quad z \ge \frac{p_i(f_i) - p_i(f_i^u)}{p_i(\bar{f}_i) - p_i(f_i^u)}, \qquad i = 1, \ldots, m$$

$$g_j(\boldsymbol{x}) \ge 0, \qquad j = 1, \ldots, p$$

$$h_k(\boldsymbol{x}) = 0, \qquad k = 1, \ldots, q$$

$$f_{i5} \ge f_i(\boldsymbol{x}) \qquad \text{(class 1-S)}$$

$$f_i(\boldsymbol{x}) \ge f_{i5} \qquad \text{(class 2-S)}$$

$$f_{i5R} \ge f_i(\boldsymbol{x}) \ge f_{i5L} \qquad \text{(class 3-S)}$$

$$f_{i5R} \ge f_i(\boldsymbol{x}) \ge f_{i5L} \qquad \text{(class 4-S)}$$

$$x_l^u \ge x_l \ge x_l^l, \qquad l = 1, \ldots, n \tag{3}$$

where α is set as a sufficiently small positive number, e.g., 10^{-6}. The vector $\boldsymbol{f}^u$ is called the ideal point (or utopia point). The components of $\bar{\boldsymbol{f}}$ are called the aspiration levels. The following settings are used to generate that Pareto design that satisfies the DM's initial preferences: $p_i(f_i^u) = 0$ and $p_i(\bar{f}_i) = 1$.

The PP method involves converting a multiobjective problem into a single-objective problem by using preference functions that capture the designer's preferences and then solving this single objective optimization for a compromise solution. The PP formulation considers the tradeoffs that exist between objectives implicitly, and generates a Pareto design that is in the preferred region of the Pareto surface. However, the PP in its current form requires that the preferences as well as the range parameters be specified a priori. Some of the limitations of using PP for multiobjective system design optimization are as follows: it 1) requires a priori selection of range parameters for each of the objective functions, 2) provides information for only one design scenario (i.e., a single Pareto solution), and 3) provides no information about the available Pareto designs in the neighborhood of the current design for tradeoff analysis and decision making.

Keeping these limitations in mind, the goal of this research is to develop an interactive physical programming (IPP) method that provides the designer with the following information at a given Pareto design for decision making: 1) Pareto sensitivity information, 2) Pareto surface representation using response surfaces, 3) tradeoff analysis and decision-making capability, and 4) Pareto visualization tool for tradeoff studies.

The Pareto sensitivity analysis and Pareto surface representation have been developed in Ref. 6 in the context of an interactive multiobjective optimization procedure (IMOOP). In this research, the concepts mentioned earlier are being implemented within graphical user interface (GUI) of the PP. The IPP is characterized by phases of decision making alternating with phases of optimization. This method empowers the designer to act as a DM at the end of each optimization. The capabilities mentioned earlier provide the designer with a formal means for design exploration around a given Pareto point. The original contributions of this research to the multiobjective optimization community are: the implementation of the Pareto sensitivity analysis, the utilization of response surface-based techniques for Pareto surface representation, the development of an iterative decision-making strategy for Pareto surface exploration, and the development of Pareto visualization tool for tradeoff studies within PP.

Pareto Sensitivity Analysis

The sensitivity analysis at a given Pareto point provides the variation in one objective given the variation in another objective (i.e., $\mathrm{d}f_i/\mathrm{d}f_j$) on the Pareto surface in a given direction. These sensitivities, which are tangent lines to the Pareto surface, are directional derivatives. Note that the Pareto surface, at a given Pareto point, has infinite tangent directions. The sensitivity analysis presented here seeks to find the sensitivity information along the principal directions (i.e., feasible descent direction of each of the objectives) in the objective function space.

At a given constrained Pareto optimal point $\boldsymbol{x}^*$, let $\boldsymbol{g}^a(\boldsymbol{x}^*)$ represent the set of active constraints (including the active bounds and excluding the active side constraints on objective functions). Let $\boldsymbol{J}$ represent the Jacobian of the active constraint set at $\boldsymbol{x}^*$. The terms of the Jacobian and the projection matrix $\boldsymbol{P}$ of the active constraint set are given by

$$\boldsymbol{J} = \nabla_x \boldsymbol{g}^a \tag{4}$$

$$\boldsymbol{P} = \boldsymbol{I} - \boldsymbol{J}^T(\boldsymbol{J}\boldsymbol{J}^T)^{-1}\boldsymbol{J} \tag{5}$$

where $\boldsymbol{P}$ represents the projected feasible directions along which the constraint set status is unchanged. Note that this projection matrix is the tangent hyperplane to the active set at $\boldsymbol{x}^*$. A feasible direction with the greatest improvement of objective f_i is obtained by projecting $\nabla_x f_i$ onto the matrix $\boldsymbol{P}$:

$$\boldsymbol{d}_{f_i}(n x 1) = \boldsymbol{P}(-\nabla_x f_i), \qquad i = 1, \ldots, m \tag{6}$$

To determine the Pareto sensitivity $\mathrm{d}f_i/\mathrm{d}f_j$ along the feasible descent direction of objective f_j, differentiate f_i and f_j with respect to $\boldsymbol{x}$:

$$\mathrm{d}f_j = \boldsymbol{d}_{f_j}^T \mathrm{d}\boldsymbol{x} \tag{7}$$

$$\mathrm{d}f_i = \boldsymbol{d}_{f_i}^T \mathrm{d}\boldsymbol{x}, \qquad i = 1, \ldots, m, \qquad i \neq j \tag{8}$$

solving Eq. (7) for $\mathrm{d}\boldsymbol{x}$ by projection:

$$\mathrm{d}\boldsymbol{x} = \left[\boldsymbol{d}_{f_j}^T \boldsymbol{d}_{f_j}\right]^{-1} \boldsymbol{d}_{f_j}^T \, \mathrm{d}f_j \tag{9}$$

Equation (9) represents the change in design variables along the feasible descent direction of objective f_j for a decrease in that objective (i.e., $\mathrm{d}f_j$). Substituting this result in Eq. (8) for $\mathrm{d}\boldsymbol{x}$ and by rearranging the terms the following expression for the tradeoff information of objective f_i along the feasible descent direction of objective f_j ($\mathrm{d}f_i/\mathrm{d}f_j$) is obtained as

$$\frac{\mathrm{d}f_i}{\mathrm{d}f_j} = \boldsymbol{d}_{f_i}^T \left[\boldsymbol{d}_{f_j}^T \boldsymbol{d}_{f_j}\right]^{-1} \boldsymbol{d}_{f_j}, \qquad i = 1, \ldots, m \tag{10}$$

Similarly, one can conduct Pareto sensitivity analysis along the feasible descent direction of each of the other objective functions. This sensitivity information can be represented in a matrix form, called the tradeoff matrix, whose ith row represents the tradeoffs required for an improvement in the ith objective (f_i):

$$T = \begin{bmatrix} 1 & \frac{\mathrm{d}f_2}{\mathrm{d}f_1} & \cdots & \frac{\mathrm{d}f_m}{\mathrm{d}f_1} \\ \frac{\mathrm{d}f_1}{\mathrm{d}f_2} & 1 & \cdots & \frac{\mathrm{d}f_m}{\mathrm{d}f_2} \\ \cdots & \cdots & \cdots & \cdots \\ \frac{\mathrm{d}f_1}{\mathrm{d}f_m} & \frac{\mathrm{d}f_2}{\mathrm{d}f_m} & \cdots & 1 \end{bmatrix} \tag{11}$$

This Pareto sensitivity information can be used to find the normal to the Pareto surface at the current Pareto design. The tradeoff between any two objective functions exists only if the corresponding off-diagonal element in the tradeoff matrix is negative. The magnitude of the tradeoff, if it exists, is given by the absolute value of the corresponding off-diagonal element. On the other hand, a positive element in any given row indicates that there is no tradeoff between these two objectives (i.e., both of them can be improved simultaneously). Note that at least one element in any given row has to be negative for a given design to be a local Pareto optimum. This condition is necessary and not sufficient for a local Pareto optimum.

Pareto Surface Representation

The sensitivity analysis presented earlier provides information in a few specified directions. The goal of this section is to represent the Pareto surface in the neighborhood of the current Pareto design by using first-order and second-order response surface approximations. This representation is useful in decision making as it provides comprehensive information about the Pareto surface and facilitates the DM's exploration of the Pareto designs. The first-order terms of the Pareto surface approximation are determined based on the tradeoff matrix (T) given in Eq. (11) and the second-order (i.e., the Hessian) terms are determined based on the Pareto data generated around the current design.

Before describing these approximations, it is necessary to mention the limitations and conditions under which they are valid. As mentioned earlier, the Pareto surface is highly nonlinear, nonsmooth, and has discontinuities. For smooth approximations to work, the active set changes should be mild (C^0 discontinuities), and for them to be valid in the entire neighborhood of the current point, there should be no nearby jumps or kinks (C^1 discontinuities) in the Pareto surface. The mathematical description of the Pareto surface in objective function space is given by

$$S(f_1, f_2, \ldots, f_m) = 0 \tag{12}$$

The first-order approximation to the Pareto surface at the current Pareto design ($\boldsymbol{x}^*$) is given by

$$\tilde{S} = \sum_{i=1}^{m} \frac{\mathrm{d}S}{\mathrm{d}f_i}\left(f_i - f_i^*\right) = 0 \tag{13}$$

$$\tilde{f}_m^1 = f_m^* + \sum_{i=1}^{m-1} \frac{\mathrm{d}f_m}{\mathrm{d}f_i}\left(f_i - f_i^*\right) \tag{14}$$

The gradients in Eq. (14) are the normals to the Pareto surface at the current Pareto point. The term $\mathrm{d}f_m/\mathrm{d}f_i$ is the change in objective f_m for a given change in f_i although keeping the other objectives constant. These terms are determined based on Eq. (11). The second-order Pareto surface approximation at the current Pareto design (x^*) is given by

$$\tilde{f}_m^2 = f_m^* + \sum_{i=1}^{m-1} \frac{\mathrm{d}f_m}{\mathrm{d}f_i}\Delta f_i + \frac{1}{2}\sum_{i,j=1}^{m-1} \Delta f_i \boldsymbol{H}_{ij} \Delta f_j \tag{15}$$

where $\boldsymbol{H}_{ij}$ is given by

$$\boldsymbol{H}_{ij} = \frac{\mathrm{d}^2 f_m}{\mathrm{d}f_i\,\mathrm{d}f_j}, \qquad i, j \neq m \tag{16}$$

Note that there are m objective functions and the second order approximation [Eq. (15)] represents one of the objectives (mth objective) in terms of the other $m - 1$ objectives. If one were to neglect off-diagonal terms and estimate only the diagonal terms of the Hessian matrix, the number of terms to be determined would be $m - 1$. On the other hand, if one were to estimate the entire symmetric Hessian matrix, the number of terms to be determined would be $m(m - 1)/2$. Note that the Pareto data to be generated (or required) are proportional to the number of terms to be determined. The second-order terms are determined based on Pareto data generated around the current design using a least-squares minimization. The Pareto data-generation method that is developed as a part of this research is explained in the next section.

Pareto Data Generation

One obvious way of generating the required Pareto data is to solve a number of CP problems (Eq. 3) with different aspiration points ($\bar{\boldsymbol{f}}_i$) around the current Pareto design. Solving a number of CP problems involves the solving of a full optimization problem a number of times. This is prohibitively expensive as it requires a large number of analysis calls for function and gradient evaluations. In order to avoid solving a large number of expensive CP problems, in this research, the approximate Pareto data are generated using a projection method that uses the gradient information available at the current Pareto design. A discussion of the details of this method follows.

The projection method essentially involves the finding of preferred Pareto points ($\boldsymbol{f}_i^*$) by projecting the aspiration points ($\bar{\boldsymbol{f}}_i$) onto the Pareto surface as shown in Fig. 2. For each aspiration point, the projection is done in two steps, the predictor step and the corrector step.

Predictor Step

This step, as the name suggests, predicts an approximate Pareto point corresponding to a given aspiration point (e.g., $\bar{\boldsymbol{f}}_1$). This step uses the first-order approximations of $f_i(\boldsymbol{x})$, $g_j(\boldsymbol{x})$, $h_k(\boldsymbol{x})$ with respect to design variables at the current Pareto design ($\boldsymbol{x}^*$). In this step, the following linear CP problem is solved to predict the design vector $\boldsymbol{x}_{1p}^*$ (shown in Fig. 2) corresponding to the aspiration point $\bar{\boldsymbol{f}}_1$.

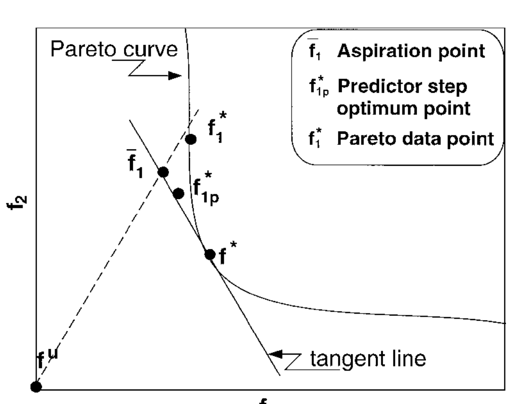

Fig. 2 Projecting the aspiration point $\bar{f}_1$ onto the Pareto curve.

$$\text{Minimize:} \quad z + \alpha \sum_{i=1}^{m} p_i[\tilde{f}_i(\boldsymbol{x})]$$

$$\text{s.t.:} \quad z \geq \frac{p_i[\tilde{f}_i(\boldsymbol{x})] - p_i(f_i^u)}{p_i[(\bar{\boldsymbol{f}}_1)_i] - p_i(f_i^u)}, \qquad i = 1, \ldots, m$$

$$\tilde{g}_j(\boldsymbol{x}) \geq 0, \qquad j = 1, \ldots, p$$

$$\tilde{h}_k(\boldsymbol{x}) = 0, \qquad k = 1, \ldots, q$$

$$x_l^u \geq x_l \geq x_l^l, \qquad l = 1, \ldots, n \tag{17}$$

where $\tilde{f}_i(\boldsymbol{x})$, $\tilde{g}_j(\boldsymbol{x})$, $\tilde{h}_k(\boldsymbol{x})$ are the linear approximations given by Eq. (18). Since approximations are being used in this step, it is necessary to conduct the optimization subject to move limits on design variables. Note that the optimum objective function values ($\bar{\boldsymbol{f}}_{1p}^*$), at the end of this step, will only be equal to the aspiration levels if there are no active constraint set switches. Moreover, the optimum design obtained at the end of this step may not be feasible. The optimum design $\boldsymbol{x}_{1p}^*$ obtained at the end of this step is projected back onto the Pareto surface by performing the corrector step explained next:

$$\tilde{f}_i(\boldsymbol{x}) = f_i^* + \nabla_{x^*} f_i(\boldsymbol{x} - \boldsymbol{x}^*), \qquad \tilde{g}_j(\boldsymbol{x}) = g_j^* + \nabla_{x^*} g_j(\boldsymbol{x} - \boldsymbol{x}^*)$$

$$\tilde{h}_k(\boldsymbol{x}) = h_k^* + \nabla_{x^*} h_k(\boldsymbol{x} - \boldsymbol{x}^*) \tag{18}$$

Corrector Step

In this corrector step, the Pareto point ($\boldsymbol{f}_1^*$) corresponding to the aspiration point, $\bar{\boldsymbol{f}}_1$, is found by projecting (or correcting) the optimum design $\boldsymbol{x}_{1p}^*$ onto the Pareto surface. This is achieved by solving a few iterations of the compromising programming problem [Eq. (3)] corresponding to aspiration point $\bar{\boldsymbol{f}}_1$. This corrector step is performed by using the generalized reduced gradient (GRG) method[11] due to its ability to maintain feasibility. Note that the GRG method needs gradient information in each iteration for the search direction calculations. In order to avoid calculating the gradient information at each iteration of the GRG method and to increase the computational efficiency, the gradient information $\nabla_{x^*}(f_i, g_j, h_k)$ available at the current Pareto design ($\boldsymbol{x}^*$) is used for search direction calculations. Note that, because the gradient information from the current Pareto design is used, the analysis routines are invoked by the optimizer only for function evaluation thus increasing the efficiency of the projection method.

Since the approximate search direction is used in each iteration of the GRG method, the Pareto data obtained by performing the corrector step may be clustered close to the current Pareto point. In other words, the Pareto data may not be well distributed in the entire range of approximation required. In such cases, it is necessary to obtain additional Pareto data points. These additional data points may be obtained by performing the above corrector step with exact gradients calculated at the beginning of each GRG iteration.

Iterative Decision-Making Strategy (IDMS)

If a given design is Pareto optimal, there is no other feasible design that improves all of the objective functions. Therefore, if the DM wants to improve some of the objective functions, it can only be done at the expense of certain other objective functions. It is generally difficult for the DM to know which objectives have to be relaxed in order for an improvement in a given objective. Moreover, in large design problems, it is often impossible for the DM to know precisely how much to change a given aspiration level in order to obtain a satisfactory solution.

Considering these difficulties, this section addresses the issue of decision making at a given Pareto design by developing an IDMS. The decision making involves a systematic exploration of the Pareto surface at a given Pareto design to learn about the available Pareto tradeoffs that exist between objective functions and to move to a preferred design. Note that the decision-making process has to be iterative and interactive in nature because the DM may want to modify his/her current preferences as he/she learns more about the available designs during the course of the IDMS.

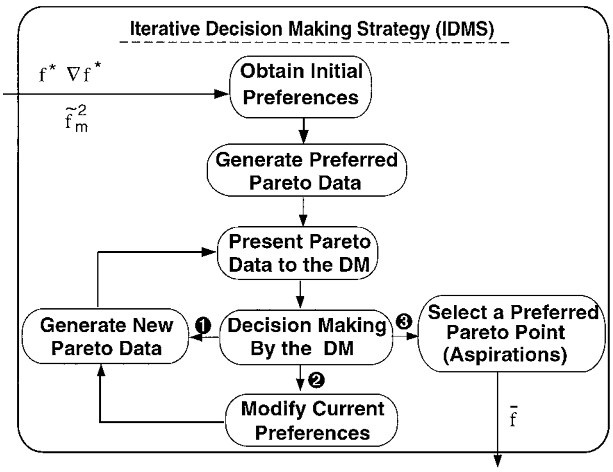

Fig. 3 Flowchart of the IDMS.

The flowchart of the IDMS is shown in Fig. 3. At the beginning of the IDMS, the DM specifies qualitative preferences, if they exist, on objective functions. For a given objective f_i, these preferences are of the form: improve f_i, sacrifice f_i, or satisfied with current f_i. Note that the DM cannot request an improvement in all of the objective functions at a given Pareto design as it is not possible to improve all of the objectives.

Once the preferences are specified by the DM, a set of approximate Pareto points is generated such that they lie on the second-order Pareto surface approximation, and satisfy the DM's current preferences. These approximate Pareto points are presented to the DM for his/her inspection. To facilitate the tradeoff studies by the DM, the approximate Pareto points are presented in the preference space (i.e., p-space) in the form of bar charts (called the Pareto visualization tool). This is explained in the Results section. After examining the points presented, the DM can choose one of the following options:

1) Generate a different set of approximate Pareto points with current preferences.

2) Modify current preferences and generate approximate Pareto points.

3) One of the points presented is satisfactory.

If the DM chooses option 1, a new set of Pareto points that are on the approximate Pareto surface are generated, and the iterative process is repeated. If the DM chooses option 2, the DM is asked to modify his/her current preferences. Once the DM modifies the existing preferences, a set of approximate Pareto points, based on the new preferences, are generated and presented for inspection. Finally, if the DM chooses option 3, the decision-making process is terminated and the final point chosen by the DM is used as an aspiration vector for the generation of a new Pareto design. The IDMS is repeated until the DM chooses one of the points to be satisfactory (i.e., option 3).

Interactive Physical Programming (IPP)

This section presents the flowchart of the IPP framework that is developed as a part of this research for multiobjective optimization in which the DM is directly involved a priori and a posteriori in decision making. The key elements in IPP are 1) PP, 2) Pareto sensitivity analysis, 3) Pareto surface approximation, 4) IDMS, and 5) Pareto visualization tool.

These concepts have been described in detail earlier. The flowchart for this procedure is given in Fig. 4. As shown in the flowchart, the DM specifies his/her initial preferences in the form of region limits defined in PP. The Pareto optimal design corresponding to these initial preferences is generated by solving a PP problem [Eq. (3)]. At the current Pareto design, a Pareto sensitivity analysis [Eq. (10)] is conducted. Pareto data in the neighborhood of the current Pareto design are generated by using the projection method. These design points coupled with the Pareto sensitivity information are used to form the second-order Pareto surface approximation at the current design [Eq. (15)]. Now the IDMS is invoked. The DM is asked to specify preferences on which a set of approximate Pareto points that satisfy his/her current preferences are generated such that

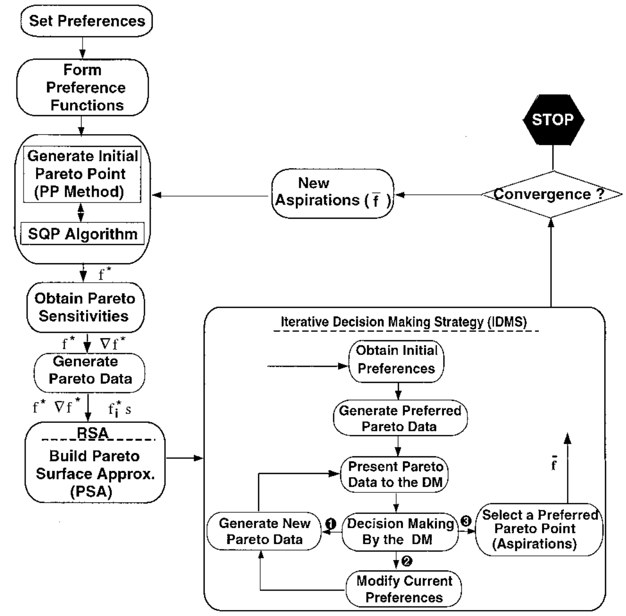

Fig. 4 Flowchart of IPP.

they are on the second-order Pareto surface approximation. These designs are presented to the DM for decision making in the form of bar charts in preference space (called the Pareto visualization tool).

At this point, the DM can choose one of the following options: generate a new set of approximate Pareto points that satisfy the current preferences, modify the current preferences, and then generate a set of Pareto points. Once the DM chooses an option, a set of approximate Pareto points that satisfy his/her current preferences are generated such that they are on the second-order Pareto surface approximation. The new set of points are presented to the DM for inspection. This iterative decision making is continued until the DM is satisfied with one of the points presented. The point chosen by the DM at the end of IDMS is used as an aspiration vector for the generation of a new Pareto point. The IPP is repeated until the DM is satisfied. Note that the procedure does not have any mathematical basis for its convergence, which is typical of any interactive multiobjective optimization procedure. All of the Pareto designs obtained are potential candidates for the final selection, and are therefore stored in a database.

Results

In this section, the IPP framework is implemented in application to two design problems. The first problem consists of a set of simple analytical expressions for its objective and constraint functions. This problem is chosen to illustrate the key features of the IPP framework. The second problem is the design and sizing of a high-performance and low-cost ten-bar structure that has weight, sustainable loads, and displacement as its objective functions. The IPP framework is implemented in Matlab 5.0.[12]

Test Problem 1

This problem has three design variables, three objective functions, and a constraint. The problem definition in standard form follows.

$$\text{Minimize:} \quad F(\boldsymbol{x}) = \{f_1(\boldsymbol{x}), f_2(\boldsymbol{x}), f_3(\boldsymbol{x})\}$$

$$\text{Subject to:} \quad g_1(\boldsymbol{x}) = 12 - x_1^2 - x_2^2 - x_3^2 \geq 0$$

$$\boldsymbol{x} \geq 0 \tag{19}$$

where the objective functions are given by

$$f_1 = 25 - \left(x_1^3 + x_1^2(1 + x_2 + x_3) + x_2^3 + x_3^3\right)/10$$

$$f_2 = 35 - \left(x_1^3 + 2x_2^3 + x_2^2(2 + x_1 + x_3) + x_3^3\right)/10$$

$$f_3 = 50 - \left(x_1^3 + x_2^3 + 3x_3^3 + x_3^2(3 + x_1 + x_2)\right)/10$$

From these expressions, it can be observed that the objectives are nonlinear functions of design variables, and the constraint is a

Table 1 DM's initial preferences (PP region limits)

			h	*D*	*T*	*U*	*H*
Criterion	Class		f_{i1}	f_{i2}	f_{i3}	f_{i4}	f_{i5}
f_1	1-S	$-\infty$	3.0	4.25	6.0	7.5	9.0
f_2	1-S	$-\infty$	3.7	7.0	9.25	11.8	12.5
f_3	1-S	$-\infty$	6.0	12.0	15.0	18.0	20.0

Table 2 Initial and optimum designs

Vector	Initial values			Optimum values		
x	1.0	1.0	1.0	1.916	2.262	1.792
F	9.4	14.2	19.0	5.708	8.486	12.106
g	9.0					

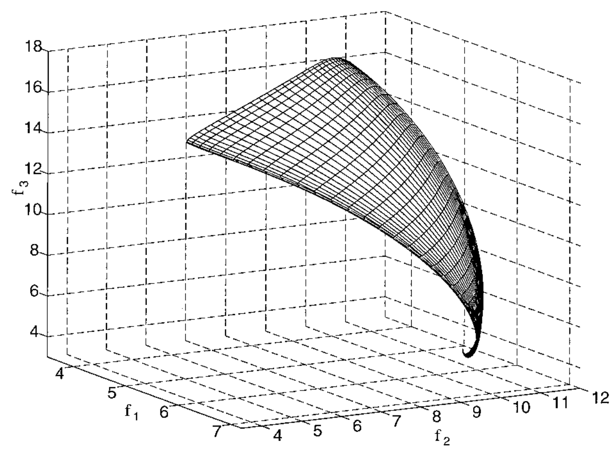

Fig. 5 Pareto surface.

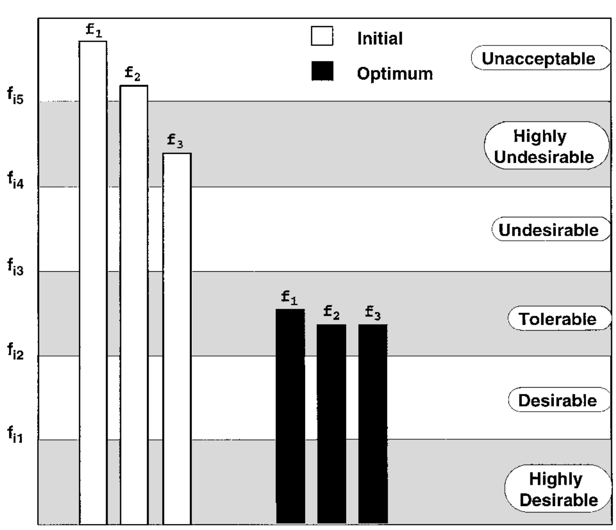

Fig. 6 Histogram of the initial and optimum design.

quadratic function of the design variables. The Pareto surface for this problem is shown in Fig. 5. The following are the steps involved in application of IPP to this three-design variable problem.

Step 1. The first step in IPP is to get the DM's initial preferences for each of the three objective functions in the form of region limits. Because there is no real DM here, the preferences are assumed to be as specified in Table 1. Once the preferences are specified, the Pareto design that satisfies these preferences is obtained by solving the IPP's optimization problem [Eq. (3)]. The initial and the Pareto design obtained are given in Table 2. The histogram of these designs is shown in Fig. 6 in terms of the DM's preferences in the preference space (i.e., p-space). It can be seen from the results that the IPP has successfully managed to move the initial design, which is unacceptable, into a tolerable (or preferred) region of the Pareto set by considering the Pareto tradeoffs that exist between objective functions implicitly.

Step 2. Once the optimum design is obtained, it is assumed here that the DM would like to explore the Pareto surface in the neighborhood of the current Pareto design for design options. This step considers the Pareto sensitivity analysis at the current design. Note that the sensitivity analysis presented here is in the objective function space (f-space) and not in the preference space (p-space). At the optimum, constraint g_1 is active. Based on Eq. (11), the tradeoff matrix is obtained as

$$T = \begin{bmatrix} 1.000 & -1.088 & -1.629 \\ -0.204 & 1.000 & -0.822 \\ -0.138 & -0.373 & 1.000 \end{bmatrix} \tag{20}$$

where the ith row indicates the sensitivity information with respect to objective function f_i along its feasible descent direction. From the tradeoff matrix, it can be seen that a decrease in any objective function from its current value is associated with a simultaneous increase in the other two objective functions (i.e., negative off-diagonal elements). The fact that each of the off-diagonal elements is negative indicates that the current point is Pareto optimal. The first-order approximation to the Pareto surface, which is determined based on the tradeoff matrix T [Eq. (20)], is given by

$$\tilde{f}_1^1 = 5.708 - [0.432 \quad 0.369] \begin{pmatrix} f_2 - 8.486 \\ f_3 - 14.106 \end{pmatrix} \tag{21}$$

Note that this first-order Pareto surface approximation is nothing but a tangent plane to the Pareto surface at the current design. The next step in IPP is to construct a second-order Pareto surface approximation at the current Pareto design.

Step 3. To obtain a second-order Pareto surface approximation, it is necessary to generate Pareto data around the current design. As explained earlier, these Pareto data are generated by projecting the aspirations that are on the first-order Pareto surface approximation onto the actual Pareto surface. In the present case, four Pareto data points are being used to estimate the second-order terms.

To generate these Pareto data around the current Pareto design, the aspiration points are chosen such that the values of $\bar{f}_2$ and $\bar{f}_3$ are at the corners of a 20% perturbed hypersquare around the current Pareto design. The value of $\bar{f}_1$ for these four aspiration points is chosen such that they lie on the first-order Pareto surface approximation [Eq. (21)]. The four aspirations points that are chosen are given in Table 3. The Pareto data corresponding to these aspiration points are obtained by using the projection method described earlier. The projection method required an average of five function calls for each Pareto data point. Note that the gradient information available at the current Pareto point ($\boldsymbol{f}^*$) has been used during the projection method. The approximate Pareto data obtained corresponding to the four aspiration points are also given in Table 3. The second-order Pareto surface approximation of f_1 in terms of f_2 and f_3, at the current Pareto design, is determined based on the Pareto data (Table 3), and is given by

$$\tilde{f}_1^2 = 5.708 - [0.432 \quad 0.369] \begin{bmatrix} f_2 - f_2^* \\ f_3 - f_3^* \end{bmatrix} - \frac{1}{2} \begin{bmatrix} f_2 - f_2^* \\ f_3 - f_3^* \end{bmatrix}^T \begin{pmatrix} -0.095 & -0.007 \\ -0.007 & -0.041 \end{pmatrix} \begin{bmatrix} f_2 - f_2^* \\ f_3 - f_3^* \end{bmatrix} \tag{22}$$

To compare the accuracy of Pareto surface approximations, the error between the actual f_1 and the f_1 values predicted by first-order and second-order Pareto surface approximations are compared at various values of f_2 and f_3 within 25% of the current Pareto design.

Table 3 Aspiration points and Pareto data

Aspirations, $\bar{f}_i$			Pareto data, f_i^*		
1	2	3	1	2	3
7.483	6.788	11.285	6.956	7.437	11.496
5.400	6.788	16.927	5.413	6.916	16.218
6.016	10.183	11.285	3.994	10.095	16.130
3.933	10.183	16.927	4.708	8.689	16.259

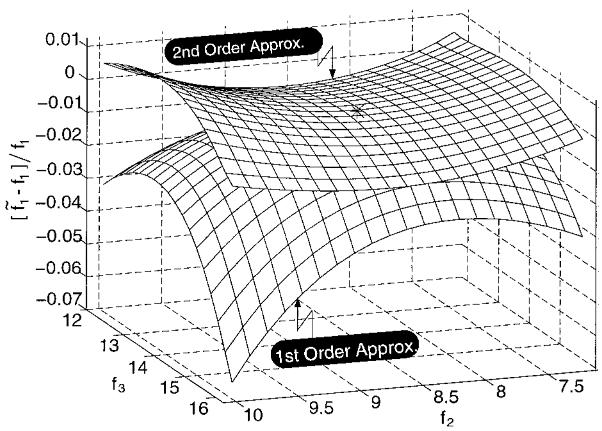

Fig. 7 Prediction errors in f_1.

The results are shown in Fig. 7. From the error plot, it can be seen that the performance of the second-order Pareto surface (error $\leq 1.0\%$) is superior when compared to that of the first-order Pareto surface (error $\leq 7.0\%$).

Step 4. This is the most important step of IPP where the DM interacts and explores the Pareto surface in the neighborhood of the current Pareto design using the IDMS. Note that the exploration is subject to move limits on objective functions as it is based on Pareto surface approximation. These move limits are determined based on the Pareto data (given in Table 3) that are used to construct the second-order Pareto surface approximation. For example, at the current Pareto design, the exploration move limits are 25% as the Pareto data are within 25% of the current Pareto design. Note that it is possible to have different move limits for different objectives depending on the Pareto data.

The Pareto data generated during this step are presented to the DM in preference function space (i.e., p space) in the form of bar charts (i.e., Fig. 6). This is called the Pareto visualization tool. This way of presenting Pareto designs to the DM clearly offers a better understanding of the tradeoff information. A quick glance at the plot clearly conveys to the DM the state of various Pareto designs. More importantly, it removes the need for the designer to directly deal with numbers, which could be difficult in the case of large multiobjective optimization problems.

Once the DM specifies his/her preferences on objective functions, the goal of this step is to efficiently generate Pareto designs that satisfy his/her preferences based on the second-order Pareto surface approximation [Eq. (22)]. Consider the following two scenarios of decision making. After inspecting the approximate Pareto designs presented in the Pareto visualization tool, let us assume that the DM wants to examine the following two scenarios:

Scenario 1. Improve f_1 and willing to sacrifice f_2 up to f_{23}.

Scenario 2. Willing to sacrifice f_1 up to f_{13}, f_2 up to f_{23}, and improve f_3.

Scenario 1. In this scenario, the DM has not specified his/her qualitative preferences on f_3 at this moment. The DM would like to inspect a set of Pareto designs or Pareto points that satisfy the current preferences prior to making decisions regarding f_3. Note that there are an infinite number of Pareto designs that satisfy the current preferences, and it would be overwhelming for the DM to inspect all of these designs. Keeping this in mind, only a set of Pareto designs that are of interest are presented to the DM. The set of four Pareto designs, given in Table 4, that satisfy the DM's current preferences are generated such that they are on the second-order Pareto surface approximation [Eq. (22)]. These four designs are presented to the DM in the Pareto visualization tool shown in Fig. 8 for ease of visualization and inspection. After inspecting the Pareto designs, the DM can accept one of these designs as a satisfactory design or ask for a different set of designs, or modify the current preferences and then ask for a set of Pareto designs. This process of generating and presenting a set of Pareto designs is repeated until convergence.

Scenario 2. In this scenario, the DM has specified his/her qualitative preferences on all of the objective functions. Here again, a set of four Pareto designs, given in Table 5 and shown in Fig. 9, that satisfy the DM's current preferences and lie on the second-order Pareto surface approximation are presented to the DM for inspection.

Once the DM chooses one of the Pareto designs presented to him/her as a potential candidate design (i.e., aspirations vector), the IDMS is terminated and a Pareto design corresponding to the aspirations vector is obtained by solving the CP problem [Eq. (3)] in preference function space. To illustrate this point, assume that after inspecting the Pareto designs presented, the DM has chosen the following design from Table 5: $\bar{f}_2 = [5.975 \quad 9.091 \quad 12.500]$ as a candidate (i.e., aspirations vector) for the generation of a new

Table 4 Preferred Pareto designs generated by the IDMS (scenario 1)

f_1	f_2	f_3
3.996	8.974	17.477
4.999	9.250	15.000
4.250	9.156	16.780
5.708	9.250	13.090

Table 5 Preferred Pareto designs generated by the IDMS (scenario 2)

f_1	f_2	f_3
6.000	9.250	12.159
5.975	9.091	12.500
6.000	8.480	13.284
5.708	9.250	13.092

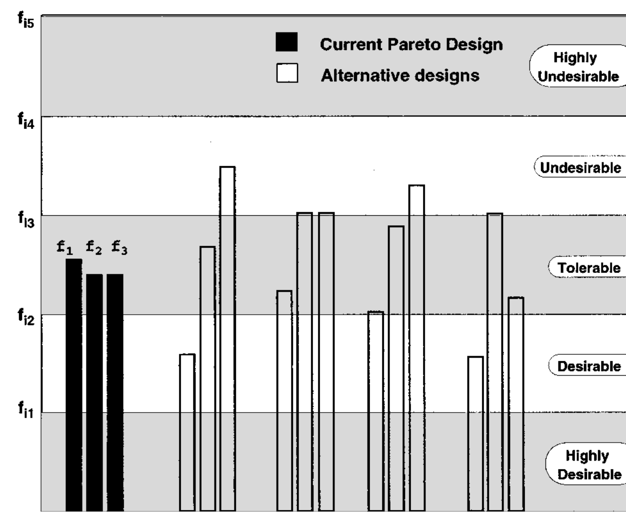

Fig. 8 Pareto visualization tool for tradeoff studies (scenario 1).

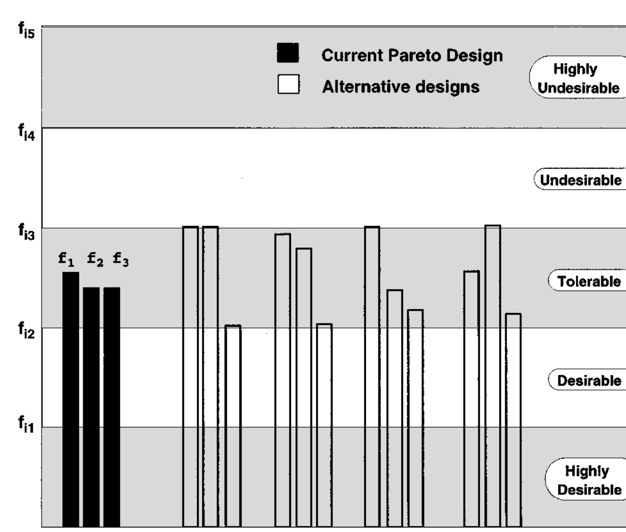

Fig. 9 Pareto visualization tool for tradeoff studies (scenario 2).

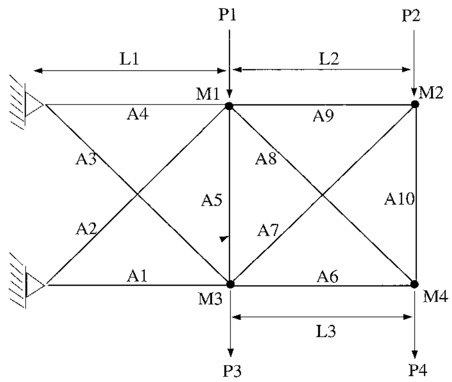

Fig. 10 High-performance, low-cost structure.

Pareto design. The new Pareto design obtained by solving a CP problem corresponding to $\bar{f}_2$ is as follows:

$$x_2^* = [1.750 \quad 2.090 \quad 2.137], \qquad f_2^* = [5.973 \quad 9.088 \quad 12.496]$$

The Pareto design f_2^* is close to the aspirations vector $\bar{f}_2$ indicating that the second-order Pareto surface approximation is accurate. From these two scenarios, it is clear that the IDMS has been able to capture the DM's local preferences effectively, and the Pareto surface approximation can be used to generate Pareto designs efficiently. The Pareto designs predicted by the approximations, around the current Pareto point, are attainable (i.e., they are accurate and are approximately on the Pareto surface). This means that the new Pareto point obtained corresponding to these aspirations is close to the aspirations. This is important for the rapid convergence of the decision-making process and for the confidence of the DM in an interactive procedure like the IPP.

Test Problem 2

The application of IPP to a structural design and sizing problem is presented. The problem is the design of a high-performance low-cost structure shown in Fig. 10. This problem was first introduced by Wujek et al.[13] It has been modified by Tappeta and Renaud[7] to fit the multiobjective optimization framework. The modified problem includes the following objective functions: minimize the structural weight W_{tot}, maximize the loads P_{1-4} the structure is capable of sustaining and minimizing the displacement of the structure (d). The goal of the optimization is to find the size and shape of a ten-bar truss that achieves a compromise among the above-mentioned three objective functions while satisfying the design constraints on minimum payload and load requirements as well as yield stress and first natural frequency constraints. The design vector in this problem is composed of the length of the rectangular first bay (L_1) and the top and bottom lengths of the outer bay (L_2, L_3), the masses (payload) placed on all the unconstrained nodes (M_{1-4}), and the areas of the truss members (A_{1-10}). The multiobjective optimization problem statement in standard form is as follows.

$$\text{Minimize:} \quad F(x) = \left\{ w_1 W_{\text{tot}}, \frac{w_2}{\sum P_i}, w_3 d \right\}$$

$$\text{Subject to:} \quad g_1 = 1 - \frac{(M_{\text{tot}})_{\min}}{\sum M_i} \geq 0$$

$$g_2 = 1 - \frac{(P_{\text{tot}})_{\min}}{\sum P_i} \geq 0$$

$$g_3 = 1 - \frac{\omega_{1,\min}}{\omega_1} \geq 0$$

$$g_{4-13} = 1 - \frac{|(\sigma_{1-10})|}{\sigma_y} \geq 0$$

$$x^l \leq x \leq x^u \qquad (23)$$

where $(M_{\text{tot}})_{\min} = 5000$ lb, $(P_{\text{tot}})_{\min} = 10{,}000$ lb, $\omega_{1,\min} = 2.0$ Hz, and $\sigma_{\text{yield}} = 14{,}000$ psi. The constants ($w_i s$) are chosen appropriately so that the objective functions are well scaled. The loads (P_{1-4}) applied to the structure are defined to be a function of the lengths of the bays (L_{1-3}) and the payload masses (M_{1-4}) placed on the structure. The displacement d is taken as the maximum absolute displacement of the top right node of the outer bay. The following are the steps involved in application of the IPP to this HPLC structural design problem.

Table 6 DM's initial preferences (PP region limits)

			h		D		T		U		H
Criterion	Class			f_{i1}		f_{i2}		f_{i3}		f_{i4}	f_{i5}
f_1	1-S	$-\infty$		3.0		5.5		6.75		10.0	13.0
f_2	1-S	$-\infty$		7.0		7.75		8.0		9.0	10.0
f_3	1-S	$-\infty$		3.0		5.0		6.0		9.5	12.4

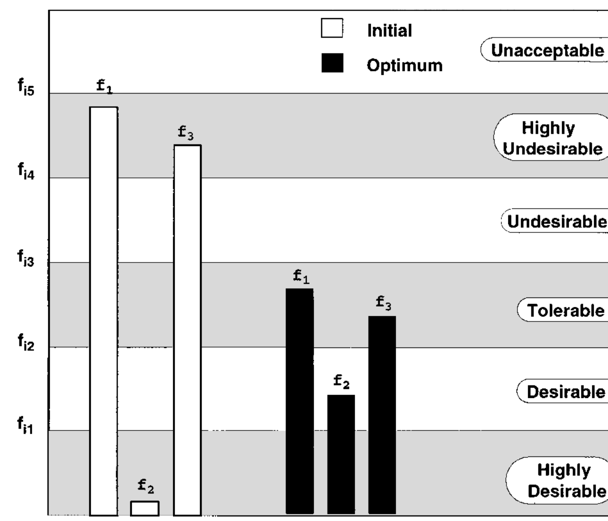

Fig. 11 Histogram of the initial and optimum design.

Step 1. The DM's initial preferences are assumed to be as specified in Table 6. The Pareto design that satisfies these preliminary preferences is obtained by solving the IPP's optimization problem [given in Eq. (3)] and is given by: $f^* = [6.356 \quad 7.298 \quad 5.314]$. The histogram of the initial and optimum designs is shown in Fig. 11 in terms of the DM's preferences. It can be seen from the results that the IPP has successfully managed to move the initial design, which is highly undesirable in some objectives, into a preferred region of the Pareto set by considering the Pareto tradeoffs that exist between objective functions implicitly.

At the optimum all the bay lengths (L_{1-3}), the first and second payloads (M_1, M_2) and two of the cross-sectional areas (A_5, A_{10}) are at their lower bounds. The frequency constraint (g_3) is the only design constraint that is active at the optimum.

Step 2. To obtain the first-order approximation to the Pareto surface at the current Pareto point, Pareto sensitivity analysis is conducted. The first-order approximation to the Pareto surface, which is determined based on the tradeoff matrix T [Eq. (11)], is given by

$$\tilde{f}_1^1 = 6.356 - [0.686 \quad 0.988] \begin{pmatrix} f_2 - f_2^* \\ f_3 - f_3^* \end{pmatrix} \qquad (24)$$

Step 3. This step considers the generation of Pareto data and building of the second-order Pareto surface approximation at the current Pareto design. Note that the Pareto surface is highly nonlinear, and it is generally difficult to get a second-order Pareto surface approximation that is accurate in the entire neighborhood of a given Pareto design. As a result, if the DM has any preferred region of the Pareto surface in which he/she would like to conduct design (or Pareto surface) exploration studies, a more accurate Pareto surface approximation in this preferred region can be obtained by generating the entire Pareto data in that region. However, note that the DM cannot change these preferences during the IDMS (invoked in step 4) and explore a region of the Pareto surface that is nonpreferred because the second-order Pareto surface approximation may not be

Table 7 Aspiration points and Pareto data

Aspirations, $\bar{f}_i$			Pareto data, f_i^*		
1	2	3	1	2	3
4.131	7.683	7.173	4.552	8.468	7.906
6.356	9.139	3.454	6.721	10.000	3.779
4.131	9.853	3.454	5.737	10.000	4.795
4.131	9.523	5.313	4.720	10.000	6.068

Table 8 Preferred Pareto designs generated by the IDMS

f_1	f_2	f_3
4.449	8.052	6.389
5.239	7.750	6.000
6.356	8.250	4.526
6.000	8.500	4.699

accurate in these nonpreferred regions of the Pareto surface. This is due to the fact that the Pareto data for constructing the second-order Pareto surface approximation is generated only in the preferred region of the Pareto surface. Thus, the DM has to be certain of his preferences at this step of IPP as he/she will not be able to change these preferences during the IDMS.

To make this point clear, consider the following scenario. After inspecting the current Pareto design (Fig. 11), assume that the DM is interested in the Pareto region in which the objective function f_1 is improved from f_1^* and he/she is willing to sacrifice f_2. This means that the DM is not interested in Pareto regions where f_1 is sacrificed to improve f_2 from f_2^*. As a result, the preferred Pareto region is given by: $f_1 \leq f_1^*$ and $f_2 \geq f_2^*$.

To generate the Pareto data in the preferred region, four aspiration points are chosen such that the values of $\bar{f}_2$ and $\bar{f}_3$ are perturbed by 35% from the current Pareto design and are on the first-order Pareto surface approximation [Eq. (24)]. The four aspirations points that are chosen are given in Table 7. The Pareto data corresponding to these aspiration points are obtained by using the projection method described earlier. The projection method required an average of 12 function calls for each Pareto data point. Note that the gradient information available at the current Pareto point ($\boldsymbol{f}^*$) has been used during the projection method. The approximate Pareto data obtained corresponding to the four aspiration points are also given in Table 7. Note that the Pareto data generated are in the preferred region of the Pareto surface. The second-order Pareto surface approximation of f_1 in terms of f_2 and f_3, at the current Pareto design, is determined based on the Pareto data (Table 7) and is given by

$$\tilde{f}_1^2 = 6.356 - [0.686 \quad 0.988] \begin{bmatrix} f_2 - f_2^* \\ f_3 - f_3^* \end{bmatrix} - \frac{1}{2} \begin{bmatrix} f_2 - f_2^* \\ f_3 - f_3^* \end{bmatrix}^T \begin{pmatrix} -0.199 & -0.092 \\ -0.092 & -0.337 \end{pmatrix} \begin{bmatrix} f_2 - f_2^* \\ f_3 - f_3^* \end{bmatrix} \tag{25}$$

To compare the accuracy of the Pareto surface approximations, the error in the f_1 predictions by first-order and second-order Pareto surface approximations are compared at various values of f_2 and f_3 within 30% of the current Pareto design. The results are shown in Fig. 12. From the error plot, it can be seen that the performance of the second-order Pareto surface (error $\lesssim$5.0%) is superior when compared to that of the first-order Pareto surface (error $\lesssim$25.0%).

Step 4. The IDMS is invoked for interactive decision making. This step is similar to the one detailed for the previous test problem. Here, the DM is presented with a set of preferred Pareto designs that are on the second-order Pareto surface approximation. The DM makes decisions after inspecting the designs presented. The details of this step are presented below.

Note that the DM has already specified his/her qualitative preferences on objectives f_1 and f_2 (in step 2). The preferences on f_3 may be made during the IDMS. The set of four Pareto designs given in Table 8 that satisfy the DM's preliminary preferences (specified in Step 2) are generated such that they are on the second-order Pareto surface approximation [Eq. (25)]. These four designs are presented to the DM in the Pareto visualization tool (shown in Fig. 13) for inspection.

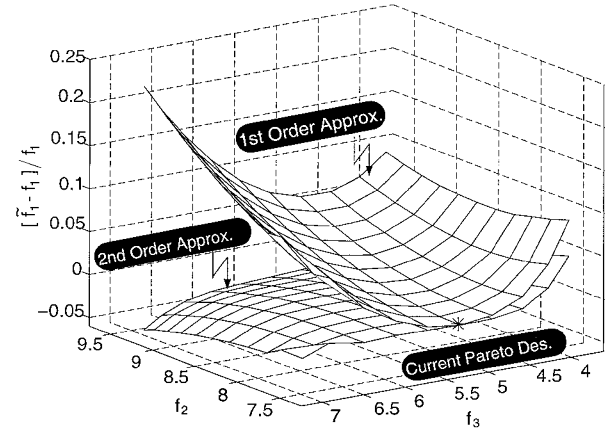

Fig. 12 Prediction errors in f_1.

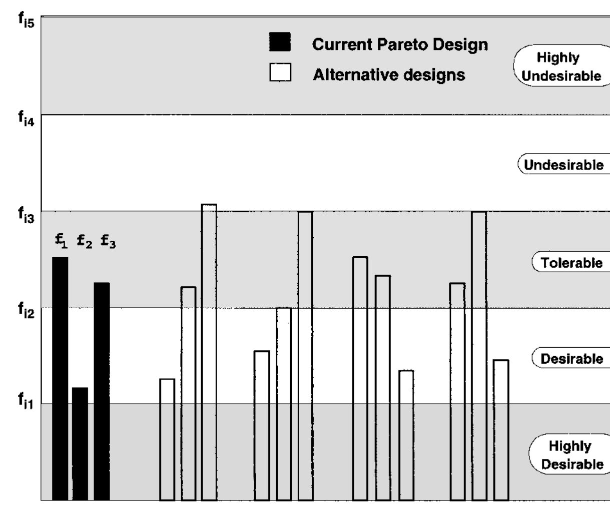

Fig. 13 Pareto visualization tool for tradeoff studies.

After inspecting these Pareto designs, the DM can accept one of these designs as a satisfactory design or ask for a different set of Pareto designs or specify his preferences on objective function f_3 and then ask for a set of preferred Pareto designs. This process of decision making and the generation of Pareto designs is repeated until the DM is satisfied with one of the designs presented.

Conclusions

In this research, the PP framework has been extended to develop an IPP framework that facilitates the designer's involvement as a decision maker in the design of multiobjective systems. The IPP provides the DM with a formal means for efficient design exploration around a given Pareto point. More specifically, the method provides the DM with Pareto sensitivity information, a second-order Pareto surface representation, an iterative decision-making strategy, and a Pareto visualization tool for tradeoff analysis and decision making.

In this study, the DM's initial preferences are captured using the PP lexicon. A second-order response surface approximation is used to represent the preferred region of the Pareto surface. An iterative decision-making strategy has been developed in which the DM learns about the existing Pareto designs and iteratively modifies his/her preferences until satisfied. To facilitate the study of tradeoffs by the DM, a Pareto visualization tool that is based on the PP lexicon is also developed.

The IPP has been successfully applied to two test problems. The results indicate that the IPP framework is effective in capturing the local preferences of the DM. The Pareto designs that reflect the DM's preferences can be efficiently generated using the IPP framework. The Pareto visualization tool allows the DM to study the existing tradeoffs between objective functions effectively. The results also indicate that the second-order Pareto surface approximation is accurate. This is important for the confidence of the DM when using an interactive framework such as IPP for obtaining a satisfactory final Pareto design in a minimal number of iterations.

Acknowledgments

This multidisciplinary research project is a joint effort between the University of Notre Dame and Northeastern University. We gratefully acknowledge the support of the National Science Foundation through Grant DMI 98-12857 for John E. Renaud and Grant DMI 97-02248 for Achille Messac. The authors would like to thank the anonymous reviewers for their insightful comments and suggestions for improving the quality of the paper.

References

[1]Eschenauer, H. A., Geilen, J., and Wahl, H. J., "SAPOP—An Optimization Procedure for Multicriteria Structural Design," *Software Systems for Structural Optimization*, edited by H. R. E. M. Hörnlein and K. Schittkowski, Vol. 110, International Series of Numerical Mathematics, 1993, pp. 207–227.

[2]Stadler, W., and Dauer, J., "Multicriteria Optimization in Engineering: A Tutorial and Survey," *Structural Optimization: Status and Promise*, edited by M. P. Kamat, Vol. 150, Progress in Astronautics and Aeronautics, AIAA, Washington, DC, 1993, pp. 209–244.

[3]Stadler, W., "Caveats and Boons of Multicriteria Optimization," *Microcomputers in Civil Engineering*, Vol. 10, No. 4, 1995, pp. 291–299.

[4]Steuer, R. E., *Multiple Criteria Optimization: Theory, Computation and Application*, Wiley, New York, 1986.

[5]Hwang, C. L., and Masud, A. S. M., *Multiple Objective Decision Making-Methods and Applications*, Springer–Verlag, Berlin, 1979.

[6]Tappeta, R. V., and Renaud, J. E., "Interactive MultiObjective Optimization Procedure," AIAA Paper 99-1207, April 1999.

[7]Messac, A., "Physical Programming: Effective Optimization for Design," *AIAA Journal*, Vol. 34, No. 1, 1996, pp. 149–158.

[8]Messac, A., and Hattis, P., "Physical Programming Design Optimization for High Speed Civil Transport (HSCT)," *Journal of Aircraft*, Vol. 33, No. 2, 1996, pp. 446–449.

[9]Messac, A., and Wilson, B., "Physical Programming for Computational Control," *AIAA Journal*, Vol. 36, No. 2, 1998, pp. 219–226.

[10]Sawaragi, Y., Nakayama, H., and Tanino, T., *Theory of Multiobjective Optimization*, Academic, Orlando, FL, 1985.

[11]Gabriele, G. A., and Beltracchi, T. J., "OPT3.2: A Fortran Implementation of the Generalized Reduced Gradient Method," *Users Manual*, Dept. of Mechanical Engineering, Aerospace Engineering and Mechanical, Rensselaer Polytechnic Inst., Troy, NY, Jan. 1988.

[12]"MATLAB Reference Guide," MathWorks, Inc., Natick, MA, Aug. 1992.

[13]Wujek, B. A., Renaud, J. E., and Brockman, J. B., "Design Driven Concurrent Optimization in System Design Problems Using Second Order Sensitivities," AIAA Paper 94-4276, Sept. 1994.

A. Chattopadhyay
Associate Editor